Antibacterial activity of the Iron-Zinc Oxide nanoparticles synthesized via electric discharge method

Fereshteh Shahbazi[1], Reza Ahmadi[1*], Mohammad Noghani[1], Gholamreza Karimi[2]

[1] Department of Materials Science and Metallurgy, Imam Khomeini International university, Qazvin, Iran
[2] Department of Mining Engineering, Imam Khomeini International university, Qazvin, Iran
*Corresponding author; Email: re.ahmadi@eng.ikiu.ac.ir

Abstract:

With the increase in diseases caused by bacterial and viral infections, the need for antibiotics has increased. On the other hand, by creating drug resistance to organicmoietiesbased antibiotics, novel antibiotics have attracted the attention of researchers.Nano-scale metal oxides are increasingly being considered for medical applications, especially as antibacterial agents.In this study, iron oxide nanoparticles (IONPs) and zinc oxide nanoparticles (ZONPs) were prepared via electrical discharge method in liquid medium by changing parameters such as wire diameter and electric current intensity. Synthesized NPs were evaluated by XRD, UV_Visible, FE_SEM, EDS, HR_TEM and TEM analyzes. Also, the antibacterial properties of these nanoparticles were evaluated in different ways against gram-positive and gram-negative bacteria.

Keywords: antibacterial, Fe_3O_4 nanoparticles, ZnO nanoparticles, E.coli, B.subtilis

1. Introduction:

Antibacterial agents play an important and influential role in various industries such as medicine, textile industry, food industry and also for disinfecting water[1-3]. Recently, metal NPshave shown unique properties in different industries and medical processes.High specific surface areaand the uniform distribution of NPs has provided them widely applications[4].Antibacterial metal nanoparticles have an effect on both gram-positive and gram-negative bacteria and cause them through various proposed mechanisms such as reactive oxygenSpecies (ROS), membrane processes and the entry of nanoparticles into the bacteria, the release of ionic metals or direct destruction of bacterial membranes[5-7]. Among the metal NPs, IONPsand ZONPshave attracted the attention of researchers due to their high antibacterial properties and cost-effectiveness[8]. There are several cost-effective methods to synthesize IONPs and ZONPs; Such as sol-gel[9], micro-emulsion[10], Thermal Decomposition[11], chemical precipitation[12], electrochemical[13], electrical arc discharge[14] and electrical wire explosion[15].The electrical discharge method is performed in liquid or gaseous medium, which has been considered by researchers because of its cost-effectiveness and eco-friendly compared to other methods[4, 16]. Metallic wireevaporates by high voltage or current intensity. The NPs are then nucleated by cooling in a liquid or gaseous medium. With this method, it is possible to produce high purity metal NPs, oxide nanoparticles as well as composite NPs[4, 14, 15].The properties and nature of nanoparticles synthesized by electrical discharge method depend on factors such as synthesis environment, wire diameter, nature of wire metal, geometric shape of wire, parameters related to electric current and applied voltage and other things[17, 18].Environmental parameters such as

pressure, pH, surfactant addition and temperature greatly influence the properties of the synthesized NPs[19, 20].

In this study, IONPs and Fe-Zn oxide NPswere synthesized at constant pH, in different current intensities and different wire diameters, by electric discharge in liquid medium[21]. Firstly, IONPswere synthesized by changing the diameter and current intensity parameters. Next, Fe-Zn OxideNPs were synthesized in optimizedcurrent intensity and diameter[22].The synthesized NPs were characterized by XRD, UV-VISIBLE,FE-SEM, TEM and HRTEM techniques. The antibacterial properties of NPsagainst two types of gram-positive and gram-negative bacteria were investigated by wet and dry methods.

2. Materials and methods:

2.2. Synthesis of Fe-Zn oxide NPs:

0.2 mm ST37 wires were connected to the anode and cathode electrodes in the electrical discharge system and the arc discharge was performed in a plastic container which containing distilled water with pH=7, the applied current was 300, 400 and 500 amps. According to the obtained results and previous researches, the current intensity of 500 amps was selected as the optimal current. Then wires with 0.3, 0.4 and 0.5mm size in diameter were employedunder 500 amps current intensity for nanoparticles synthesis. In the next step, theST37 wires were dipped into molten Zn. The Zn-coated ST37 wireswere placed between anode and cathode, and then were connected to 80 V DC power. With starting electrical discharge process, the atoms evaporate and then cool rapidly in a liquid medium to form oxide NPs. Fig.1. shows theschematic of electric discharge method process and Table 1 summarized codes of samples.

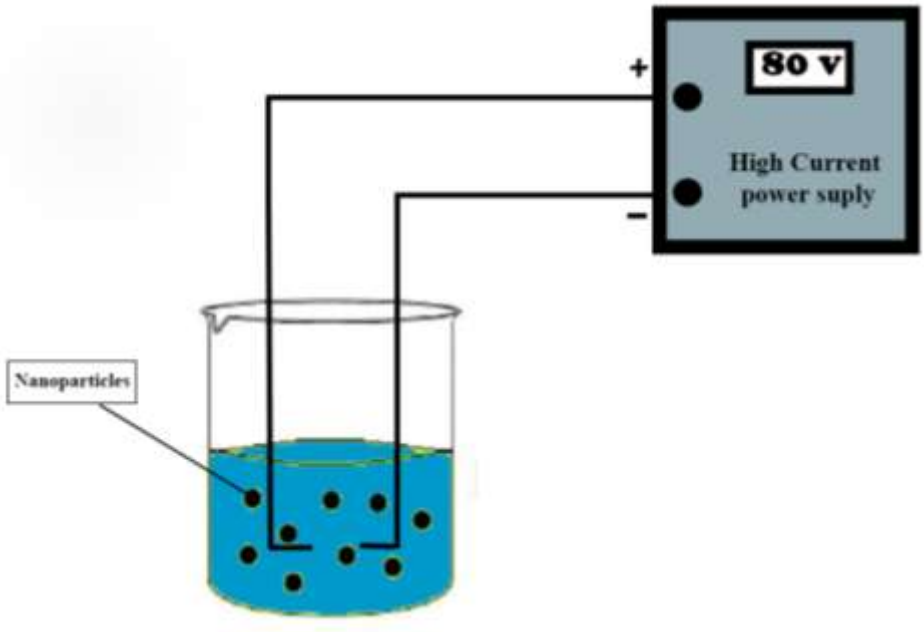

Fig. 1.Schematic of electric discharge method process.

Table 1. Specifications of synthesized samples prepared via electric discharge method in distilled water with pH=7

Sample code	Current Intensity (A)	Diameter (mm)
S01	300	0.2
S02	400	0.2
S03	500	0.2
S04	500	0.3
S05	500	0.4
S06	500	0.5
S07	500	0.2

2.3. Characterization of Fe-Zn oxideNPs:

Synthesized samples were characterized usingX-ray diffractometer(XRD, modelPANalytical with Cu K_{α}radiation of1.54060 Å ,voltage 40 kV, current intensity 40 mA and step size 0.026˚,The range of 2theta was 5 - 80˚C),UV-Vis spectroscopy (usingUV-1800 spectrophotometer), field emission scanning electron microscopy (FESEM, Model MIRA3TESCAN-XMU) equipped with energy dispersive spectroscope (EDS) , transmission electron microscopy(TEM modelLeo 912 AB) and High-resolution transmission electron microscopy (HR-TEM FEI TECNAI F20) For structural andmorphological analysis.

2.4. Antibacterial assay:

To determine the effectiveness of a nanoparticle as an antibacterial agent, experimental techniques are used that measure bacterial survival after exposure to nanoparticles. In 2006, the Institute for Clinical and Laboratory Standards (CLSI) published a document entitled "Analysis and Presentation of Antimicrobial Sensitivity Test Data" which sets out the standards required for antibacterial testing. Gram-positive and gram-negative bacteria may react differently to antibacterial nanoparticles. Therefore, studies often include at least one gram-positive species and one gram-negative species to determine antibiotic efficacy[23, 24].

2.4.1. Specifications of culture medium and bacteria:

LB broth and agar powders (QUELAB Germany) were used to prepare liquid and solid culture media for bacteria, respectively. Müller-Hinton Broth (MHB) culture medium (QUELAB Germany) was also used to evaluate the minimum inhibitory concentration (MIC). The studied bacteria were gram-negative Escherichia coli MHD5 and gram-positive Bacillus subtilis.

2.4.2. Growth curve analysis:

The antibacterial evaluation of the prepared nanoparticles was firstperformed by determining the optical density (OD).To prepare the liquid culture medium, 1.75 g of LB powder was poured into 50 ml of distilled water in an Erlenmeyer flask and placed in an autoclave at 121.5 ° C and 1.5 atmospheres for 20 minutes. Both bacteria were then inoculated separately into culture medium and placed in an incubator shaker at 37 ° C to suspend the bacterium equivalent to the 0.5 McFarland standard be prepared from any of the bacteria. Then, by adding equal amounts of bacterial suspension and adding different amounts of nanoparticles to the liquid culture medium, 4 samples with various nanoparticle concentrations of 156, 312, 625 and 1250 ppm were prepared. The samples were then placed in an incubator-shaker at 37 ° C and after each 2-hour period, the optical density at 600 nm was measured by the Spectro UV-VIS UVD-3200.The control samples used were not exposed to nanoparticles.

2.4.3. Minimum Inhibitory Concentration (MIC):

To ensure the obtained antibacterial results, the antibacterial effects of the Iron Oxide and Fe-Zn Oxide nanoparticles were evaluated using standard dilution method (CLSI M07-A8).

To prepare the liquid culture medium, 1.05 g of MHB powder per 50 ml was poured into distilled water in an Erlenmeyer flask and placed in an autoclave at 121.5 ° C and 1.5 atmospheres for 20 minutes. Each bacterium was then inoculated into the culture medium separately to obtain a bacterial suspension equivalent to the half McFarland standard. 100 microliters of freshly prepared culture medium was poured into each 96-well plate well. Then 100 microliters of nanoparticle suspension was poured into the first row wells and dilution was performed from top to bottom in all wells. Then 100 microliters of the bacterial suspension was added to each cell. Two replicates were placed for each sample. One column was placed for positive control and one column for negative control. Also, one column for each sample was placed as a control sample that contained only culture medium and nanoparticles.The plates were covered with parafilm and left for 24 hours in the incubator-shaker at 37 ° C. After incubation, 40 µl of tetrazolium salt (MTT) with a concentration of 0.2 mg/ml was added to each well and placed at room temperature for 15 minutes.Growth of bacteria in wells with purple or pink appearance is determined. If the growth of bacteria is stopped, the corresponding well will appear colorless.which The concentration of that well is considered as the amount of MIC. Finally, the plate was examined with an ELISA reader with a wavelength of 600 nm. All steps related to this test were performed under a microbial hood.

3. Results and discussion:

3.2. NPs characterizations:

3.2.1. X-ray diffraction:

XRD patterns of IONPs shown in fig.1. As can be seen,the XRD patterns reveal the characteristic diffraction peaks of cubic Fe_3O_4 (ICDD no. 01-088-0315) and cubicFe (ICDD no. 01-087-0722), respectively[8, 25]. The XRD pattern related to the S07 sample (table 1) is presented in fig.2which exhibit diffraction peaks of hexagonalZnO (ICDD no. 01-079-0205) and

cubic $ZnFe_2O_4$ (ICDD no. 01-089-1010), respectively[1, 26, 27]. The average crystallite size of the all samples which was calculated using Scherrer's formula are presented in Table 2.

Increasing the electric current intensity increases the driving force needed to create finer nuclei of nanoparticles, the result is nanoparticles with smaller grain sizes. On the other hand, nanoparticles can form and grow both directly from plasma and from existing solid nuclei. High current intensity and high cooling rate probably lead to the formation of nanoparticles with smaller granulation[22, 28, 29].

As the wire diameter decreases and the resulting particle size decreases, the percentage of oxide phase increases. Oxidation of metal nanoparticles depends on the particle size. Oxidation is a chemical reaction and chemical reactions take place on the surface; So in order to continue the reaction, more levels must be provided for the reaction. The smaller the particle size, the greater the amount of surface atoms; Therefore, as the diameter decreases, the percentage of surface atoms that have access to oxygen due to water evaporation increases, so as the wire diameter decreases and the particle size decreases, the percentage of oxide phase increases[30, 31].As the oxide phase increases, the antibacterial property intensifies.

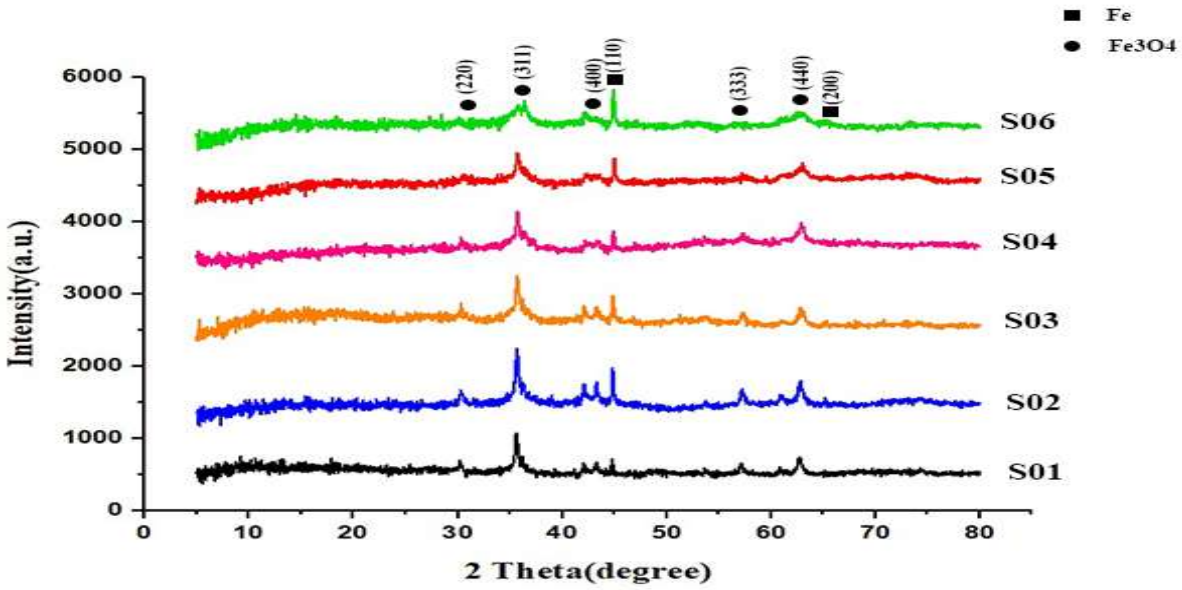

Fig. 1.XRD pattern of the iron oxide NPs prepared by the electric discharge in liquid.

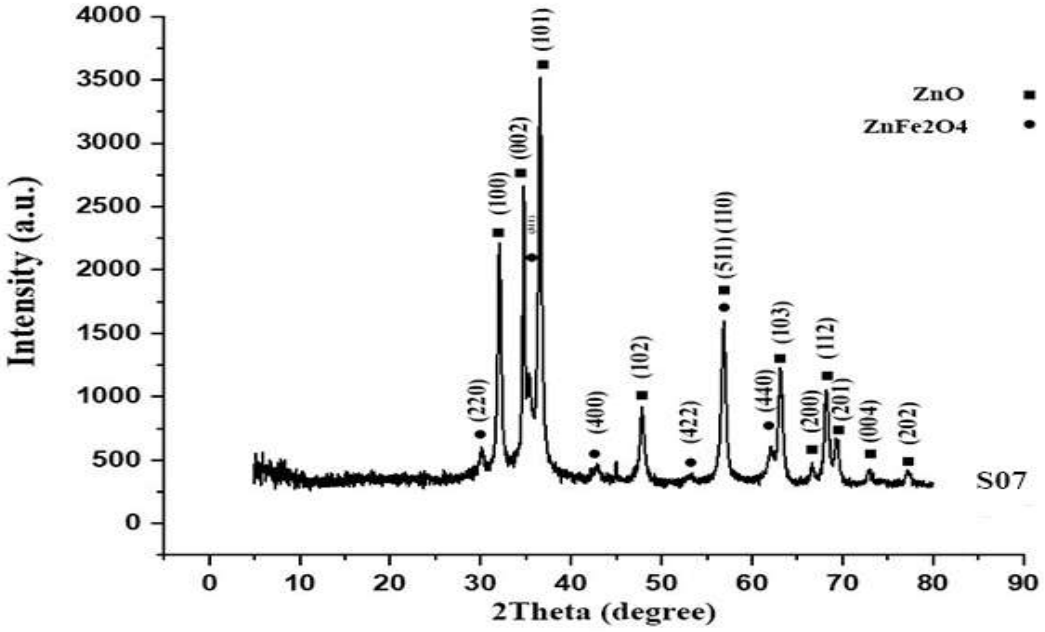

Fig. 2.XRD pattern of the Fe-Zn oxideNPs prepared by the electric discharge in liquid.

The weight percentage of each phase was calculated using Rietveld method.The results are shown in Table 2. It is clear that increasing the electric current and decreasing the diameter has increased the oxide phase. Also, the percentage of metal phase in the sample with a larger diameter is higher than other samples. In other words, as the particle size increases, the metal phase increases[32].

Table 2. Oxide and metal phase of nanoparticles.

Sample	Oxide phase (%) Fe_3O_4	Metal phase (%) Fe	Oxide phase (%) ZnO	Oxide phase (%) $ZnFe_2O_4$
S01	89	11	_	_
S02	90	10	_	_
S03	93	7	_	_
S04	91	9	_	_
S05	88	12	_	_
S06	85	15	_	_
S07	_	_	65	35

3.2.2. UV-Visible:

the UV-Visible spectraof IONPs and ZONPs are shown in fig.3. As can be seen,IONPs had an absorption peak in the range of 200 nm. The particle size and surface area of nanoparticles affect the absorption peak intensity.ZONPs had two absorption peaks in the range of 300 and 350nm which are related to ZnO and ZnFe2O4, respectively[33, 34].

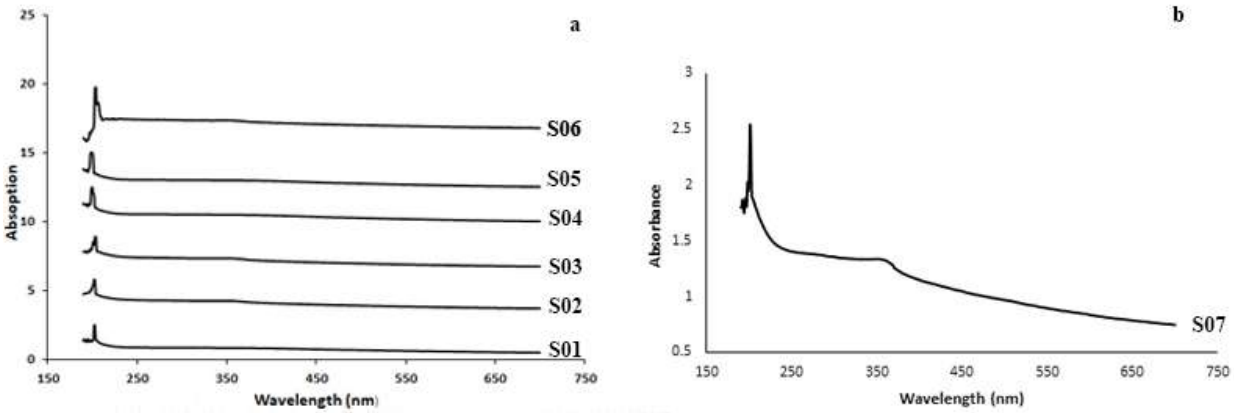

Fig. 3.UV-VISspectra of a) iron oxide nanoparticles and b) Fe-Zn nanoparticles.

3.2.3. Field emission scanning electron microscopy:

Scanning electron microscopy images are shown in Figure 4. It can be clearly seen that the iron oxide nanoparticles are completely uniform and spherical in shape. However, in the image related to the Fe-Znsample particles in rod shaped and needle-shaped are seen, which is due to the presence of zinc oxide nanoparticles.FESEM images are taken from a powder sample, and also because of the magnetic nature of iron oxide nanoparticles, the aggregationof nanoparticles and the formation of clusters has been done to a large extent[16, 21, 35]. The average particle size of the samples are given in Table 3.

In the liquid media, in contrast to gaseous media, the size of nanoparticles decreases with increasing the current intensity. As the current intensity increases, the energy input to the wires increases, and fine-grained melt buds are formed during electrical discharge, and due the high cooling rate of these fine particles, nanoparticles with smaller size are produced[21, 30, 36].

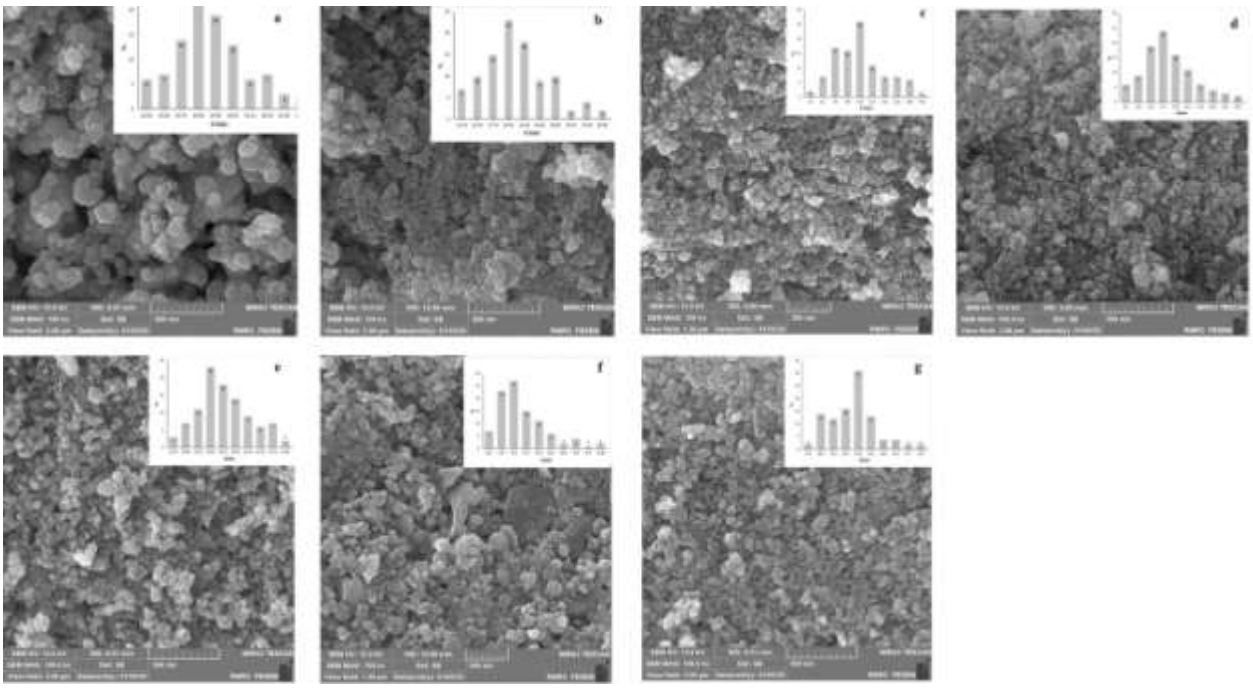

Fig. 4.FESEM images of: a)S01, b)S02, c)S03, d)S04, e)S05, f)S06 and g)S07samples.

Table 3: The average crystallite size and the average particle size of the samples according to the XRD and SEM data.

Sample	The average crystallite size (nm) (XRD)	The average particle size (nm) (SEM)
S01	17	35.85
S02	10.45	20.25
S03	8	10.3
S04	27.24	17.7
S05	29.32	26.25
S06	30.45	35.5
S07	18.46	30.9

3.2.4. TEM and HR-TEM:

Figure 5 shows the transmission electron microscope images of the synthesized samples. As can be seen, the synthesized iron oxidenanoparticles have a spherical and uniform morphology. With increasing current intensity from 300 amps to 500 amps, the average particle size has decreased

from 26.50 nm to 11.25 nm. Also, by reducing the wire diameter from 0.5 mm to 0.2 mm, the average particle size has decreased from 33.50 nm to 11.25 nm. In addition, the images show the core-shell structure.The core contains pure iron and the shell contains iron oxide[27, 37, 38].

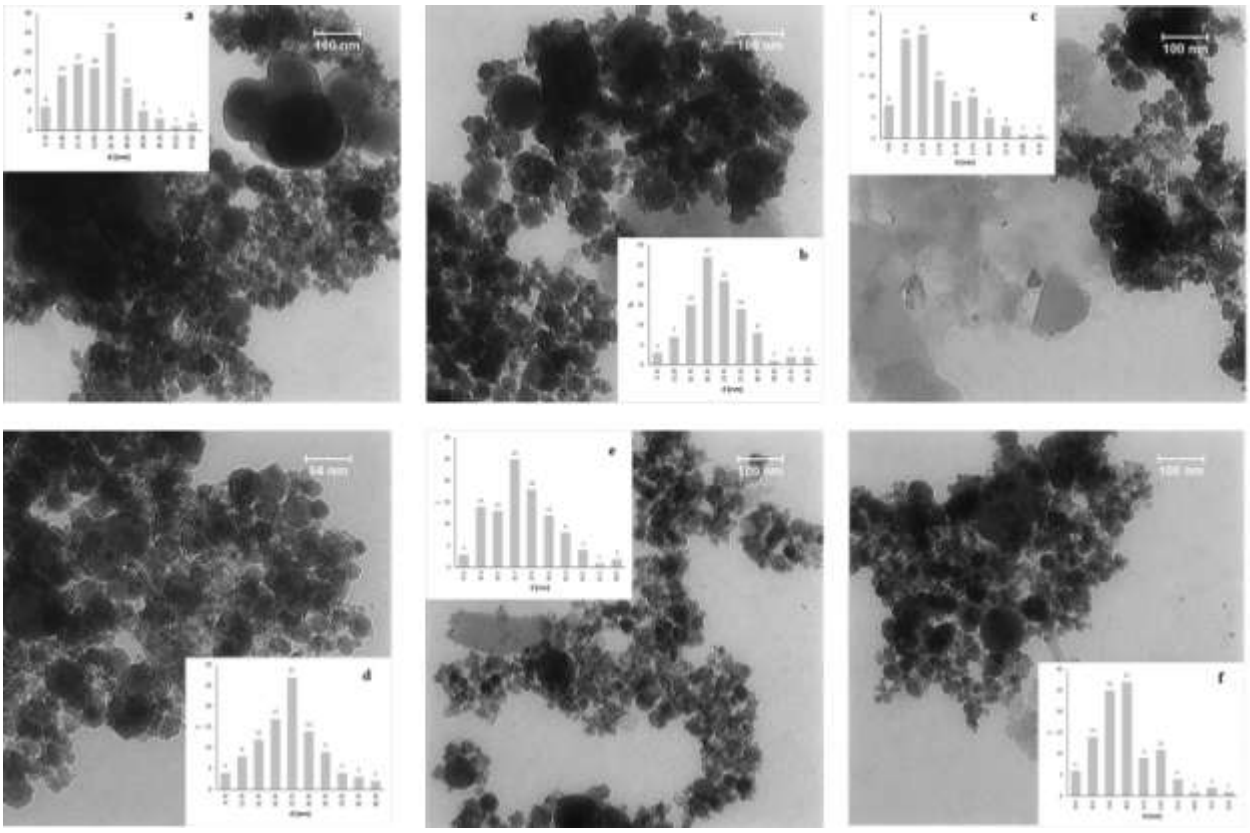

Fig. 5.TEM images of samples: a)S01, b)S02, c)S03, d)S04, e)S05, f)S06.

Fig.6. a and b show the TEM images of Fe-Zn nanoparticles. As can be seen, zinc oxide nanoparticles with a rod structure are seen. The average particle size is in the range of 20 nanometers. The core-shell structure is also clearly seen in the images. Also Fig.6. c and d present the SAED pattern and HR-TEM images Respectively[39].

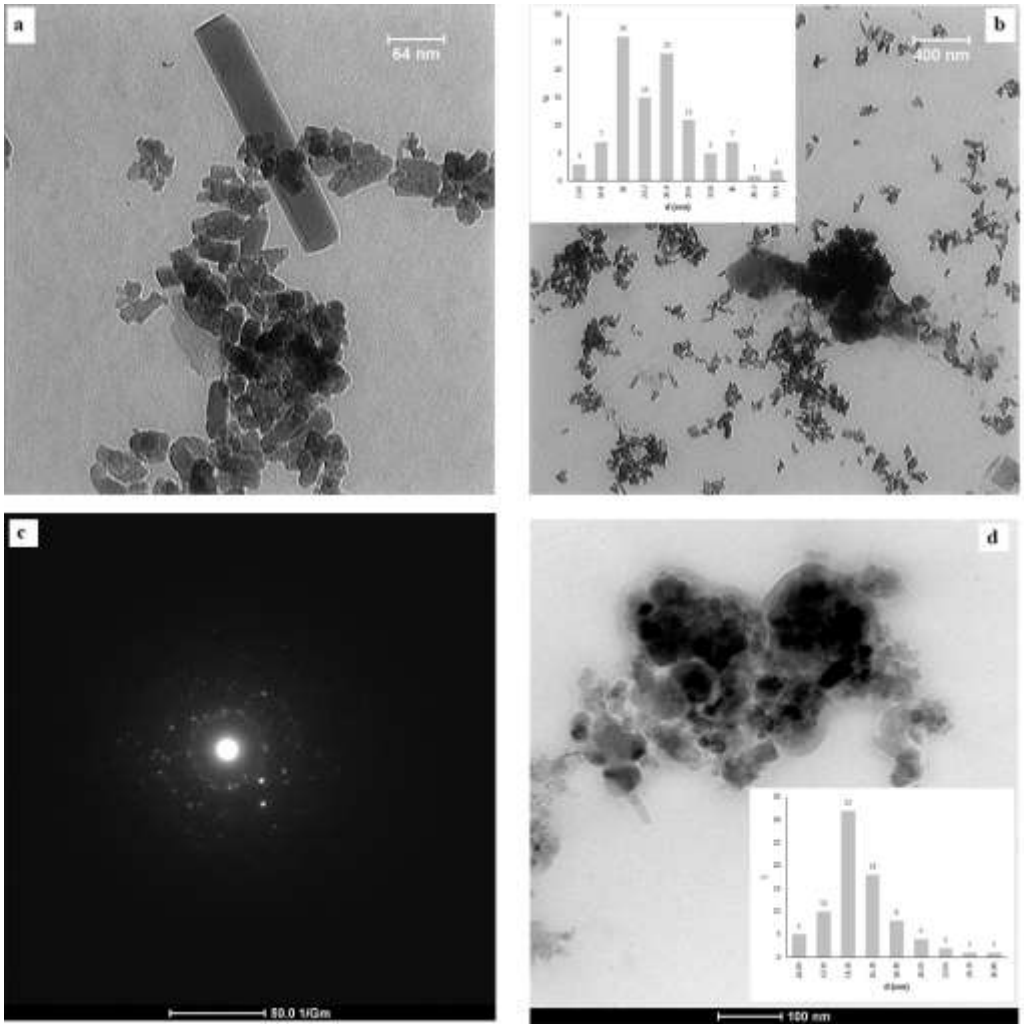

Fig. 6.a and b)TEM images of Fe-Zn NPs, c) SAED pattern, d)HRTEM image of Fe-Zn NPs.

3.3. NPs antibacterial activity:

3.3.1. Growth curve analysis:

Figure 7 and 8reveal the antibacterial activity of iron nanoparticles against both bacteria. The best result is obtained in the S03 and S07 samples, which have the lower average particle size (according to SEM and XRD images) due to the higher current intensity.

in each chart, bacterial growth is reduced or completely inhibited by increasing the concentration. This phenomenon can be exacerbated bythe interaction between bacteria and nanoparticles and thus the activation of antibacterial mechanisms. The effective mechanism for antibacterial effect of the iron oxide nanoparticles is the ROS production process as well as the reaction of Fe^{2+} with oxygen to produce hydrogen peroxide. Eventually, H2O2 reacts with iron through the Fenton process to produce hydroxyl radicals that damage biological molecules[1, 26, 40].

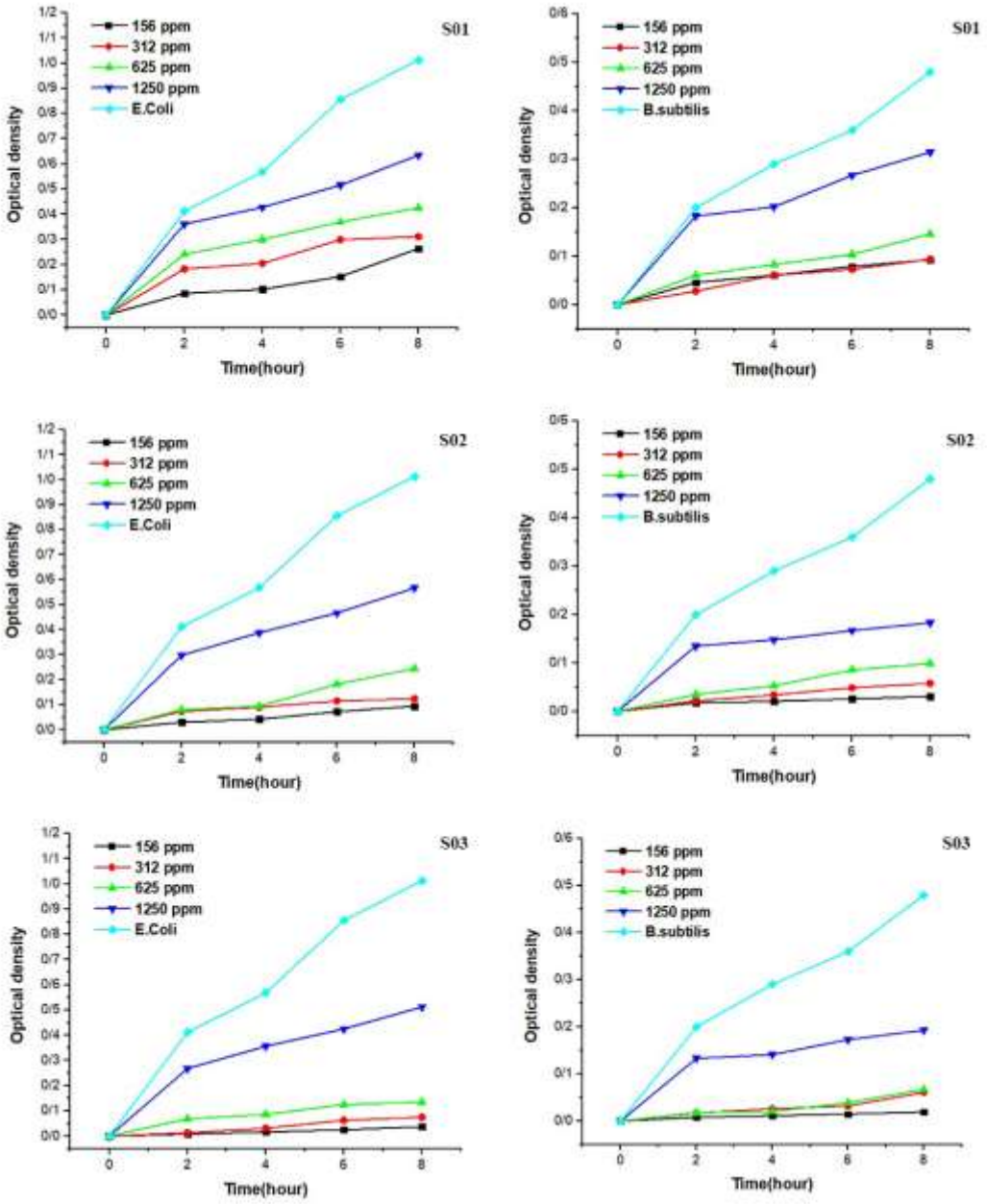

Fig. 7.Bacterial growth curve in the presence of synthesized nanoparticles.

In the case of sampleS06, it is clear that it has little effect on inhibiting bacterial growth due to the presence of large nanoparticles (according to the SEM and XRD results) as well as the low percentage of Fe_3O_4 in this sample. Researches has shown that the antibacterial effect of Fe_3O_4 is greater than other iron compounds due to its greater oxygen supply as a good source for oxidative stress reactions.

The S07 sample showed high antibacterial properties compared to both bacteria. These results are due to the synergistic effect of the presence of iron oxide and zinc oxide simultaneously and thus activating more antibacterial mechanisms. The mechanism of action of iron oxide

nanoparticles is the electrostatic interaction between nanoparticles and bacteria as well as the production of reactive oxygen species. The effective mechanisms for zinc oxide can be expressed as electrostatic interaction between nanoparticles and bacteria, production of reactive oxygen species and ion release[4, 40, 41].

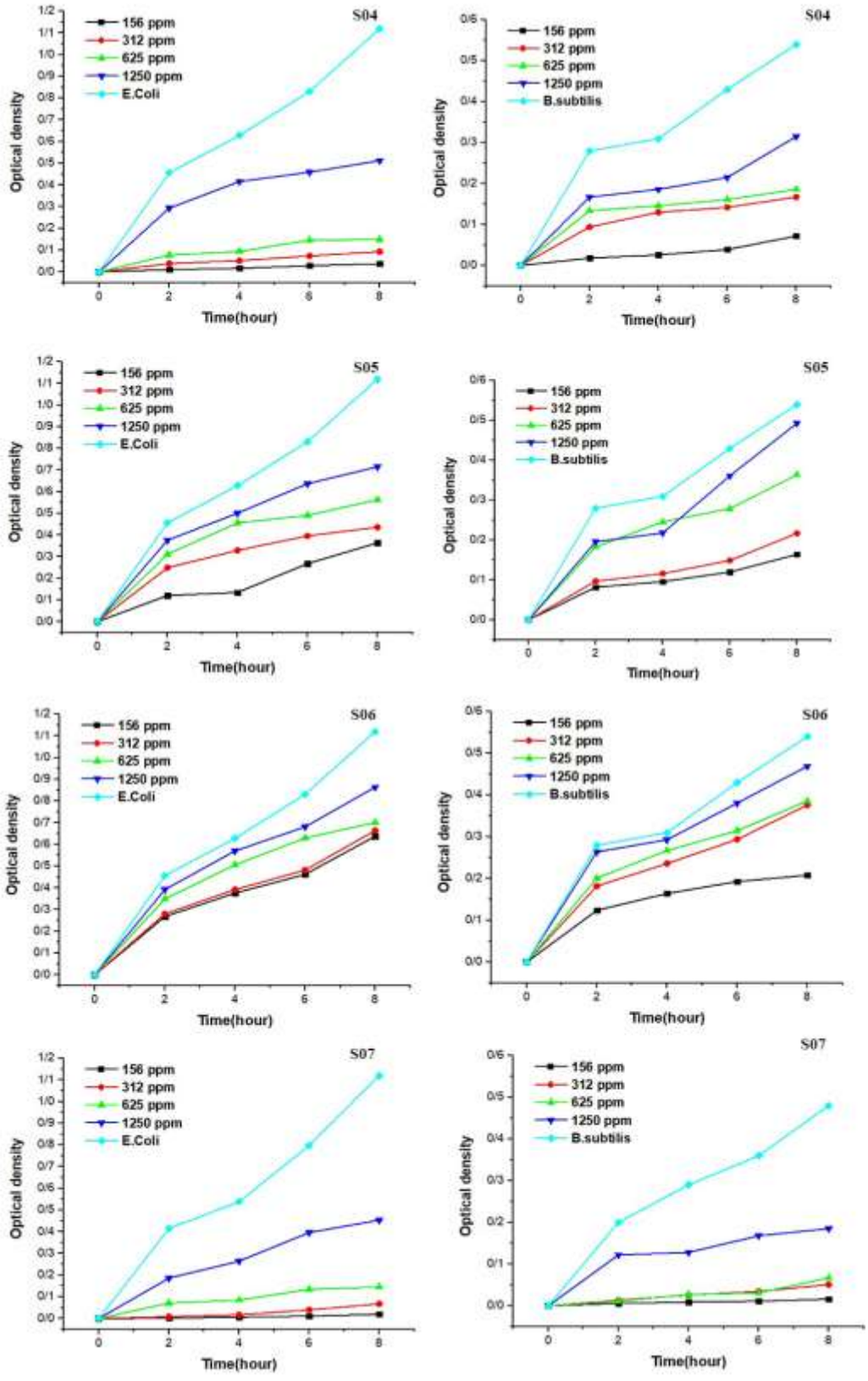

Fig. 8.Bacterial growth curves in the presence of synthesized nanoparticles.

3.3.2. Minimum Inhibitory Concentration (MIC):

The results of this study are collected in Tables4 and 5. As can be seen, the iron-zinc oxide sample showed the best performance and at concentrations higher than 312.5 µ g / ml and the bacterial growth was completely stopped.

Simultaneous activation of antibacterial mechanisms of iron oxide and zinc oxide nanoparticles has created a synergistic effect in stopping the growth of bacteria. In the case of sample S06, even at the highest concentration, despite the positive effect, but complete cessation of growth is not seen. The large size of the nanoparticles has reduced the possibility of penetration into the bacterial cell and as a result is less effective[5, 40, 42].

Table 4: the result of MIC method for E.Coli.

Concentration(µg/ml)	S01	S02	S03	S04	S05	S06	S07	E.Coli
10000	-	-	-	-	-	0.0125	-	1.42
5000	-	-	-	-	-	0.03	-	1.491
2500	-	-	-	-	0.064	0.132	-	1.524
1250	-	-	-	-	0.1335	0.223	-	1.463
625	0.119	0.1425	0.05	0.1895	0.2625	0.406	-	1.403
312.5	0.1835	0.26	0.1245	0.2425	0.3455	0.601	0.0015	1.515
156.25	0.2245	0.3975	0.1685	0.357	0.4265	0.8875	0.102	1.468
78.125	0.3335	0.434	0.223	0.432	0.725	1.13	0.175	1.526

Table 5: the result of MIC method for B.Subtilis.

Concentration(µg/ml)	S01	S02	S03	S04	S05	S06	S07	B.Subtilis
10000	-	-	-	-	-	0.0125	-	0.91
5000	-	-	-	-	-	0.1065	-	0.9
2500	-	-	-	-	0.1015	0.1745	-	0.94

1250	0.099	0.072	0.006	0.0765	0.164	0.228	-	0.87
625	0.131	0.1255	0.1185	0.1455	0.269	0.421	-	0.96
312.5	0.157	0.24	0.1625	0.208	0.306	0.606	-	0.88
156.25	0.2435	0.3765	0.1825	0.348	0.4575	0.825	0.1205	1.1
78.125	0.309	0.354	0.2125	0.381	0.6125	1.029	0.1645	1.15

Fig.9. show the antibacterial effect of nanoparticles against E.Coli and B.Subtilis bacteria by MIC method, respectively. According to these diagrams, with increasing current intensity at constant diameter, the antibacterial effect is improved and also by decreasing the wire diameter at constant current, the antibacterial activity of the samples is increased. Finally, based on the results obtained in the MIC method the bacterial strain of E.Coli is more sensitive than B.Subtilis[1, 43, 44].

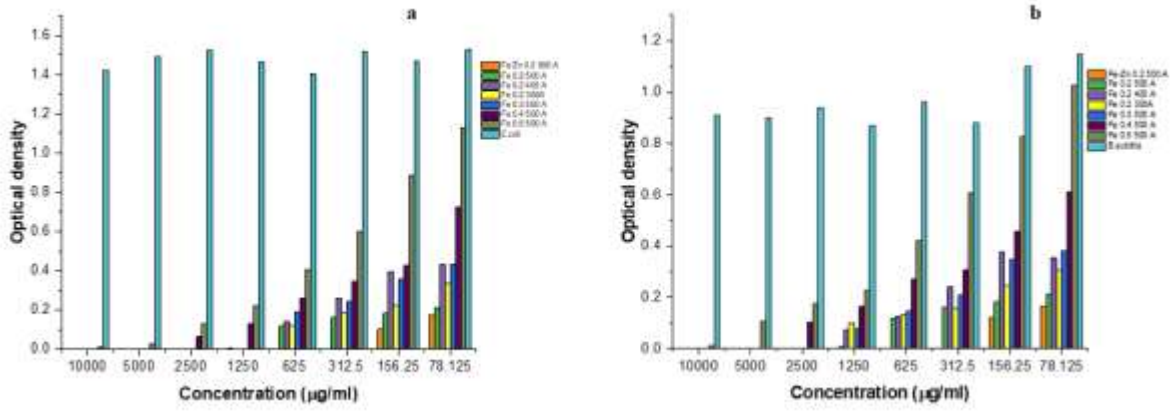

Fig. 9. Graphical results of antibacterial test by MIC method for a)E.Coli, b)B.subtilis.

4. Conclusions:

In this study, iron oxide and iron-zinc oxide nanoparticles were synthesized by electric discharge method by controlling the parameters of electric current and wire diameter. The prepared samples were microstructurally analyzed by XRD, FESEM, UV-VISIBLE, TEM and HRTEM; The results showed that reducing the wire diameter and increasing the current have a positive effect on reducing the size of nanoparticles.Growth curve and minimum inhibitory concentration methods were used to evaluate the antibacterial properties of nanoparticles against gram-positive and gram-negative bacteria. Both bacteria showed sensitivity to nanoparticles, Fe-Zn nanoparticles showed the highest antibacterial activity.

Acknowledgments

Not applicable

Authors' contributions

FS: Nanoparticles Synthesis, Antibacterial tests, Writing the manuscript. RA: Supervision, Project design. MN: Writing the manuscript, preparing the synthesis system. GK: Materials characterization. All authors read and approved the final version of the manuscript.

Funding

Not applicable

Availability of data and materials

The datasets used and characterizations performed during this study are available from the corresponding author on reasonable request.

Declarations

Ethics approval and consent to participate

Not applicable

Competing interests

The authors declare no competing interests.

Consent for publication

Not applicable

Author details

[1, 2 & 3] Department of Materials Science and Metallurgy, Imam Khomeini International university, Qazvin, Iran.
[4] Department of Mining Engineering, Imam Khomeini International university, Qazvin, Iran.

References:

1. Bhushan, M., et al., *Facile synthesis of Fe/Zn oxide nanocomposites and study of their structural, magnetic, thermal, antibacterial and cytotoxic properties.* Materials Chemistry and Physics, 2018. **209**: p. 233-248.
2. Lewis, K., *Platforms for antibiotic discovery.* Nature Reviews Drug Discovery, 2013. **12**(5): p. 371-387.
3. Aminov, R.I., *The role of antibiotics and antibiotic resistance in nature.* Environ Microbiol, 2009. **11**(12): p. 2970-88.
4. Shahriyari, F., et al., *Synthesis and characterization of Cu-Sn oxides nanoparticles via wire explosion method with surfactants, evaluation of in-vitro cytotoxic and antibacterial properties.* Advanced Powder Technology, 2020. **31**(6): p. 2337-2347.
5. Hajipour, M.J., et al., *Antibacterial properties of nanoparticles.* Trends in Biotechnology, 2012. **30**(10): p. 499-511.
6. Vidic, J., et al., *Pure and multi metal oxide nanoparticles: Synthesis, antibacterial and cytotoxic properties.* Journal of Nanobiotechnology, 2016. **14**.

7. Lemire, J., J. Harrison, and R. Turner, *Antimicrobial activity of metals: Mechanisms, molecular targets and applications.* Nature reviews. Microbiology, 2013. **11**.
8. Zhang, W., et al., *Bacitracin-Conjugated Superparamagnetic Iron Oxide Nanoparticles: Synthesis, Characterization and Antibacterial Activity.* Chemphyschem : a European journal of chemical physics and physical chemistry, 2012. **13**: p. 3388-96.
9. Gupta, A.K. and M. Gupta, *Synthesis and surface engineering of iron oxide nanoparticles for biomedical applications.* Biomaterials, 2005. **26**(18): p. 3995-4021.
10. Malik, M., M. Wani, and M. Hashim, *Microemulsion method: A novel route to synthesize organic and inorganic nanomaterials. 1st Nano Update.* Arabian journal of chemistry, 2011. **5**.
11. Lu, A.-H., E.L. Salabas, and F. Schüth, *Magnetic Nanoparticles: Synthesis, Protection, Functionalization, and Application.* Angew. Chem., Int. Ed., 2007. **46**: p. 1222.
12. Nazari, M., et al., *Synthesis and characterization of maghemite nanopowders by chemical precipitation method.* Journal of Nanostructure in Chemistry, 2014. **4**(2): p. 99.
13. Elrouby, M., A.M. Abdel-Mawgoud, and R.A. El-Rahman, *Synthesis of iron oxides nanoparticles with very high saturation magnetization form TEA-Fe(III) complex via electrochemical deposition for supercapacitor applications.* Journal of Molecular Structure, 2017. **1147**: p. 84-95.
14. Kheradmand, E., H. Delavari, and R. Poursalehi, *The Effect of Dissolved Oxygen in Arc Medium on Crystal Structure and Optical Properties of Iron Based Nanoparticles Prepared via Dc Arc Discharge in Water.* Procedia Materials Science, 2015. **11**: p. 695-699.
15. Song, K., et al., *Magnetic iron oxide nanoparticles prepared by electrical wire explosion for arsenic removal.* Powder Technology, 2013. **246**: p. 572-574.
16. Lerner, M.I., et al., *Synthesis of Al nanoparticles and Al/AlN composite nanoparticles by electrical explosion of aluminum wires in argon and nitrogen.* Powder Technology, 2016. **295**: p. 307-314.
17. Raffi, M., et al., *Investigations into the antibacterial behavior of copper nanoparticles against Escherichia coli.* Annals of Microbiology, 2010. **60**(1): p. 75-80.
18. Sundaram, R., et al., *Electrical performance of lightweight CNT-Cu composite wires impacted by surface and internal Cu spatial distribution.* Scientific Reports, 2017. **7**.
19. Lee, Y.S., et al., *Effect of ambient air pressure on synthesis of copper and copper oxide nanoparticles by wire explosion process.* Current Applied Physics, 2012. **12**(1): p. 199-203.
20. Park, E., H.W. Park, and J. Lee, *Synthesis of hierarchical copper oxide composites prepared via electrical explosion of the wire in liquids method.* Colloids and Surfaces A: Physicochemical and Engineering Aspects, 2015. **482**: p. 710-717.
21. Buazar, F., A. Cheshmehkani, and M.Z. Kassaee, *Nanosteel synthesis via arc discharge: media and current effects.* Journal of the Iranian Chemical Society, 2012. **9**(2): p. 151-156.
22. Kassaee, M., F. Buazar, and E. Motamedi, *Effects of Current on Arc Fabrication of Cu Nanoparticles.* Journal of Nanomaterials, 2010. **2010**.
23. Horvat, R., *Review of Antibiogram Preparation and Susceptibility Testing Systems.* Hospital Pharmacy, 2010. **45**: p. S6-S9.
24. Seil, J.T. and T.J. Webster, *Antimicrobial applications of nanotechnology: methods and literature.* Int J Nanomedicine, 2012. **7**: p. 2767-81.
25. Wasfi, A.S., H.R. Humud, and N.K. Fadhil, *Synthesis of core-shell Fe3O4-Au nanoparticles by electrical exploding wire technique combined with laser pulse shooting.* Optics & Laser Technology, 2019. **111**: p. 720-726.
26. Farbod, M., A. Movahed, and I. Kazeminezhad, *An investigation of structural phase transformation of monosize γ-Fe2O3 nanoparticles fabricated by arc discharge method.* Materials Letters, 2012. **89**: p. 140-142.

27. Salamat, S., H. Younesi, and N. Bahramifar, *Synthesis of magnetic core–shell Fe3O4@TiO2 nanoparticles from electric arc furnace dust for photocatalytic degradation of steel mill wastewater.* RSC Advances, 2017. **7**(31): p. 19391-19405.
28. Taccogna, F., *Nucleation and growth of nanoparticles in a plasma by laser ablation in liquid.* Journal of Plasma Physics, 2015. **81**.
29. Faraji, M., R. Poursalehi, and M. Aliofkhazraei, *The Effect of Surfactant on Colloidal Stability, Oxidation and Optical Properties of Aluminum Nanoparticles Prepared via Dc Arc Discharge in Water.* Procedia Materials Science, 2015. **11**: p. 684-688.
30. Chernavskii, P.A., et al., *Oxidation of metal nanoparticles: Experiment and model.* Russian Journal of Physical Chemistry B, 2007. **1**(4): p. 394-411.
31. Hedberg, Y.S., et al., *Electrochemical surface oxide characteristics of metal nanoparticles (Mn, Cu and Al) and the relation to toxicity.* Electrochimica Acta, 2016. **212**: p. 360-371.
32. Ahmadi, S., et al., *Green Synthesis of Magnetic Nanoparticles Using Satureja hortensis Essential Oil toward Superior Antibacterial/Fungal and Anticancer Performance.* BioMed Research International, 2021. **2021**: p. 8822645.
33. Xu, Q., et al., *Hollow ZnFe2O4/TiO2 composites: High-performance and recyclable visible-light photocatalyst.* Journal of Alloys and Compounds, 2015. **641**: p. 110-118.
34. Vidhya, K., et al., *Structural and optical characterization of pure and starch-capped ZnO quantum dots and their photocatalytic activity.* Applied Nanoscience, 2014. **5**: p. 235-243.
35. Shabgard, M.R. and A.F. Najafabadi, *The influence of dielectric media on nano-structured tungsten carbide (WC) powder synthesized by electro-discharge process.* Advanced Powder Technology, 2014. **25**(3): p. 937-945.
36. Karakoti, A.S., et al., *Preparation and Characterization Challenges to Understanding Environmental and Biological Impacts of Nanoparticles.* Surf Interface Anal, 2012. **44**(5): p. 882-889.
37. Predescu, A., et al., *Synthesis and characterization of dextran-coated iron oxide nanoparticles.* Royal Society Open Science, 2018. **5**: p. 171525.
38. Lari, L., S. Steinhauer, and V.K. Lazarov, *In situ TEM oxidation study of Fe thin-film transformation to single-crystal magnetite nanoparticles.* Journal of Materials Science, 2020. **55**(27): p. 12897-12905.
39. Das, S., et al., *Synthesis, morphological analysis, antibacterial activity of iron oxide nanoparticles and the cytotoxic effect on lung cancer cell line.* Heliyon, 2020. **6**(9): p. e04953.
40. Arakha, M., et al., *Antimicrobial activity of iron oxide nanoparticle upon modulation of nanoparticle-bacteria interface.* Scientific Reports, 2015. **5**(1): p. 14813.
41. Yusof, N.A.A., N.M. Zain, and N. Pauzi, *Synthesis of ZnO nanoparticles with chitosan as stabilizing agent and their antibacterial properties against Gram-positive and Gram-negative bacteria.* International Journal of Biological Macromolecules, 2019. **124**: p. 1132-1136.
42. Rajabi, S.K. and S. Sohrabnezhad, *Fabrication and characteristic of Fe3O4@MOR@CuO core-shell for investigation antibacterial properties.* Journal of Fluorine Chemistry, 2018. **206**: p. 36-42.
43. Riaz, M., et al., *In Vitro antibacterial activity of Ta2O5 doped glass-ceramics against pathogenic bacteria.* Journal of Alloys and Compounds, 2018. **764**: p. 10-16.
44. Armijo, L.M., et al., *Antibacterial activity of iron oxide, iron nitride, and tobramycin conjugated nanoparticles against Pseudomonas aeruginosa biofilms.* Journal of Nanobiotechnology, 2020. **18**(1): p. 35.